Am J Nucl Med Mol Imaging 2026;16(2):100-106
www.ajnmmi.us /ISSN:2160-8407/ajnmmi0170081

*Original Article*

# Calibration and prediction of results after failed injection in SPECT renal dynamic imaging

Jianping Zhang[1*], Jiaqi Zhang[4*], Miaomiao Zhang[2], Ruxin Lei[2], Kai Zhang[1], Xingru Pang[1], Xiaoxue Tian[1], Luxi Yang[5], Zhen Cao[3], Jiangyan Liu[1], Jicheng Li[1]

*[1]Department of Nuclear Medicine, The Second Hospital and Clinical Medical School, Lanzhou University, Lanzhou 730030, Gansu, China; [2]The Second Clinical Medical School of Lanzhou University, Lanzhou 730030, Gansu, China; [3]Siemens Healthineers Ltd., Shanghai 200120, China; [4]Department of Medical Imaging, The No. 2 People's Hospital of Lanzhou, Lanzhou 730030, Gansu, China; [5]Key Laboratory of Digestive System Tumors of Gansu Province, The Second Hospital and Clinical Medical School, Lanzhou University, Lanzhou 730030, Gansu, China. [*]Equal contributors.*

Received November 18, 2025; Accepted March 8, 2026; Epub April 15, 2026; Published April 30, 2026

**Abstract:** To predict bilateral renal curves and glomerular filtration rate (GFR) following unsuccessful tracer injection in SPECT renal dynamic imaging using a Transformer model, thereby obviating the need for repeat examinations. We retrospectively studied patients who underwent repeat imaging post-extravasation (2015-2025). Patient height, weight, serum creatinine, urea, uric acid, and renal dynamic curves were used as inputs to develop a Transformer deep learning model for calibrating curves and predicting GFR. Following injection extravasation during SPECT renal dynamic imaging, the proposed model achieved a high overall alignment with the ground truth curves (Median $R^2$>0.93). However, performance variability was observed, with a small subset of outliers showing poor fit (minimum $R^2$<0) due to complex noise artifacts. For the left kidney, the model achieved an $R^2$ of 0.9288, with 91.78% of predictions falling within a clinically acceptable tolerance of ±5 ml/min of the ground truth. Similarly, for the right kidney, the $R^2$ reached 0.9216, with an accuracy rate of 93.15% based on the same tolerance threshold. It is important to note that the ±5 ml/min criterion was used strictly as a statistical threshold to define 'clinical accuracy' and did not involve any modification of the predicted values. In conclusion, a Transformer model can accurately calibrate and predict bilateral renal curves and GFR values after injection extravasation in SPECT renal dynamic imaging, potentially enhancing clinical workflow efficiency and diagnostic accuracy.

**Keywords:** Renal dynamic imaging, transformer model, GFR, calibration and prediction

## Introduction

Single-Photon Emission Computed Tomography (SPECT) renal dynamic imaging is a valuable modality for assessing renal blood perfusion, location, size, and morphology. This technique also enables a comprehensive evaluation of glomerular filtration rate (GFR), bilateral renal blood flow, renal parenchymal function, and urinary tract obstruction [1], providing clinically meaningful diagnostic information. Consequently, SPECT renal dynamic imaging is widely regarded as the gold standard for assessing split renal function [2]. However, its measurements are influenced by multiple factors, including bolus injection quality, renal depth measurement, hydration status, radioactive drug dose determination, and delineation of the renal region of interest (ROI) [3]. Among these, bolus administration quality of the radiopharmaceutical is a key determinant. To obtain accurate renal dynamic images, time-activity curves, and GFR values, the radioactive agent technetium-99m diethylenetriaminepentaacetic acid ($^{99m}$Tc-DTPA) must be rapidly injected intravenously as a "bolus" maintaining an aggregated "mass" that passes through the perfusion area without diffusion [4]. The quality of this bolus injection directly affects bilateral renal perfusion and GFR values, thereby impacting the diagnosis of renal function [5]. Given the stringent requirements for bolus administration, injection failure necessitates allowing the radionuclide to be excreted and decayed on the same day, with re-imaging scheduled for the next day [6]. This increases patient radiation exposure, prolongs hospital stay, wastes radioactive drugs, and delays treatment [7, 8]. Therefore, avoiding such re-examinations is a pressing clinical challenge.

In recent years, Artificial Intelligence (AI) has become increasingly crucial in disease prediction [9]. The Transformer model excels at constructing models for long time series: it automatically identifies key target information via the attention mechanism, enabling efficient extraction of image features from imaging data and accurate prediction model development [10-12]. Consequently, it holds strong potential for predicting GFR values and bilateral renal curves after failed injections in SPECT renal dynamic imaging. This study aimed to use Transformer deep learning for multi-modal modeling (including time-series curves, anthropometric features-instead of "human body characteristics", a more academic term, clinical indicators, and injection-related information) on large datasets of failed SPECT renal dynamic imaging injections. The goal is to calibrate post-extravasation renal curves

and predict GFR values, thereby improving clinical efficiency and diagnostic accuracy, and resolving the long-standing issue of next-day re-examinations.

## Materials and methods

*Patient characteristics*

A total of 275 patients who underwent SPECT renal dynamic imaging at our hospital from January 2015 to May 2025 and required re-examination the next day due to $^{99m}$Tc-DTPA extravasation were included. Among them, 146 were male and 129 were female, with a mean age of (48.6 ± 17.2) years. Inclusion criteria: (1) Patients with injection site counts accounting for >5% of total counts and a bimodal radioactive peak in the curve; (2) Patients with undiagnosable images due to drug extravasation who consented to re-examination. Exclusion criteria: (1) Children <10 years or adults >85 years; (2) Patients with a single kidney or post-renal transplantation; (3) Patients lacking clinical indicators, anthropometric features, or injection-related information; (4) Inpatients who underwent renal function blood tests within 3 days prior to the examination; (5) Patients with repeated failed re-examinations on the next day.

*Imaging methods*

Siemens SPECT Symbia T16 and GE Xeleris 860 systems were used for image acquisition, and curves from the two devices were normalized following sensitivity calibration. Drug preparation: A 2.5 ml syringe was used to aspirate fresh technetium solution, which was then injected into DTPA. After mixing, 111-185 MBq of the radiopharmaceutical (volume: 0.5-1 mL) was administered according to the patient's weight, with radiochemical purity >95%. Drug measurement: The syringe containing the radionuclide tracer was placed on a prefabricated rack near the center of the SPECT detector for full-syringe count acquisition for 1 min. After dynamic image acquisition, the patient's injection site and post-injection syringe were separately placed at the detector center to measure injection site counts and residual syringe counts for 1 min.

Patient preparation: Patients were advised to avoid renal venography or contrast-enhanced renal CT within 2 days prior to the examination. They were advised to ensure adequate sleep. Consume a light diet on the examination day, drink 300-500 mL of water 30 minutes pre-examination, and empty the bladder prior to imaging.

Image acquisition: The patient lay supine on the examination table with a fixed position to ensure that both renal regions and the bladder remained within the detector's field of view. The sleeve on the injection side was kept loose, and a thick, straight vein was prioritized for injection. The imaging agent was administered as a bolus into one cubital vein, with simultaneous initiation of bilateral renal dynamic image acquisition for 21 minutes. Specifically: Blood perfusion imaging: 1 frame per second for 60 consecutive seconds; Renal dynamic function imaging: 1 frame per minute for 20 consecutive minutes. Acquisition parameters: Low-energy general collimator, energy peak = 140 keV, window width = 20%, matrix = 64×64, zoom = 1.26.

*Image processing*

A single physician with professional training in nuclear medicine and more than 15 years of clinical experience independently performed image analysis. Image analysis was conducted using the built-in software of the SPECT renal dynamic imaging workstation. First, the patient's height and weight were entered. The ROI technique was used to uniformly delineate the contours of the left/right kidneys, abdominal aorta, and background ROI on the posterior image; Bilateral renal blood perfusion curves, function curves, and split renal GFR values (used the Gates method) were generated using the instrument's standard processing protocol.

*Data collection*

Patient demographics (age and gender) and laboratory data (serum creatinine, urea, and uric acid) measured within the preceding 3 days were retrieved from the Hospital Information System (HIS) using each patient's admission number. Subsequently, regions of interest (ROIs) were delineated on the image processing workstation to obtain full-syringe radioactivity counts, empty-syringe radioactivity counts, and injection-site radioactivity counts.

Time-radioactivity count curves of the left kidney, right kidney, and background at 0.5-1230 seconds, as well as the GFR values of the bilateral kidneys, were collected. Time-radioactivity count datas from the SPECT workstation exported directly to Microsoft Excel, while other information was entered manually. A database was established, containing time-radioactivity counts, anthropometric features, clinical lab indices, and injection-related information of patients with injection extravasation. This database was subsequently divided into an injection extravasation group and a normal bolus injection group.

*Transformer model establishment*

*Model architecture design:* A Transformer-based renal function prediction model was designed with the following structure: Input Layer: Time-series inputs were mapped to a fixed dimension (d_model = 32) via a linear projection layer, while static features were mapped to 16 dimensions through a fully connected layer. Transformer Encoder: Comprising 2 Transformer encoder layers, each equipped with 4 attention heads (nhead = 4), a feed-forward network with a dimension of 64 (dim_feedforward = 64), and batch_first = True to enable batch processing. Output Layer: The Transformer output was concatenated

with the static feature output and mapped to the target dimension through a final fully connected layer. The model was run on a GPU (if available), with the Adam optimizer (learning rate = 0.001) and Mean Squared Error (MSE) as the loss function.

Given the sample size (N = 275) relative to the complexity of renal physiological features, we implemented a lightweight Transformer encoder with 2 layers and 4 attention heads. This shallow architecture was chosen to prevent overfitting, ensuring the model learns generalizable features rather than memorizing training noise.

Regarding Positional Encoding (PE), we adopted a task-specific strategy. For the Curve Calibration module, PE was omitted because the input and output sequences share identical temporal alignment; the attention mechanism focuses on point-to-point amplitude correction, where explicit positional indices on irregular time points introduced unnecessary noise. Conversely, for the GFR Prediction module, explicit PE was retained, as the regression of functional parameters (e.g., Tmax, T1/2) is strictly dependent on the absolute temporal position of the curve features.

*Establishment of curve calibration model after injection extravasation:* We constructed a multi-modal Transformer-based time-series model. Inputs included both extravasation and non-extravasation data, comprising full time-series sequences (time-radioactivity counts for the left kidney, right kidney, and aorta) and static features (e.g., height, weight, serum creatinine, urea, uric acid). The model architecture is as follows: Time-series embedding: Linear projection to d_model = 128, Transformer Encoder: 2 layers, 4 attention heads, dropout = 0.2, ReLU activation, Static feature embedding: Fully connected (FC) layer to 128 dimensions, Fusion: Concatenation → FC (256→128) → Dropout → Output layer, Positional encoding: Not used (irregular time points), Sequence length: 220 (resampled/aligned); Features per time step: 3 (left kidney, right kidney, aorta); Training details: Adam optimizer (lr = 0.001), MSE loss, batch size = 32, 1500 epochs, no early stopping. Inputs were standardized using StandardScaler; outputs were inverse-transformed for evaluation.

*Establishment of GFR prediction model after injection extravasation:* Patients' height, weight, serum creatinine, urea, uric acid, and renal dynamic curve data were used as input sequences, with GFR values as the output. Data were preprocessed to remove background noise and to exclude outliers in GFR. A Transformer model with positional encoding was used, trained via 5-fold cross-validation (100 epochs per fold), and the optimal model was saved. Model accuracy was statistically defined based on a tolerance threshold of ±5 ml/min between the predicted and actual GFR, as detailed in the Evaluation Metrics section.

*Model evaluation and optimization*

A total of 275 patients who underwent a next-day re-examination after injection extravasation during renal dynamic imaging were included. Model performance was evaluated using 5-fold cross-validation (5-fold CV) on the full dataset, with each fold randomly split into training/validation sets (80%:20%). Final metrics report the mean ± standard deviation across folds. Specifically, the training set comprised 220 cases for model training and parameter fitting; the validation set comprised 55 cases for hyperparameter tuning, model selection, and monitoring for overfitting.

Multiple metrics were used to comprehensively evaluate the performance of the proposed Transformer model in addressing failed injections in SPECT renal dynamic imaging. Five-fold cross-validation was applied to assess model performance, including regression task metrics such as Mean Squared Error (MSE), Mean Absolute Error (MAE), $R^2$, and accuracy. Scatter plots of predicted versus actual values were generated to analyze the deviation distribution of model predictions. The model was iteratively optimized to enhance its robustness and generalization capability.

## Results

*Prediction results of extravasation curves in SPECT renal dynamic imaging*

Based on the extravasation curve prediction model for SPECT renal dynamic imaging, we separately evaluated the left and right kidneys of Sample 6 (**Figure 1**) and Sample 15 (**Figure 2**) with respect to perfusion and functional time-activity curves. The specific results are as follows:

Prediction Results for the Perfusion Curve (A): For the left kidney, MSE = 63.71, MAE = 6.18, and $R^2$ = 0.93 - indicating excellent consistency between predicted and actual values, with the model exhibiting a good fit. For the right kidney, MSE = 107.71, MAE = 8.66, and $R^2$ = 0.99 - demonstrating an extremely high fit for the right kidney's perfusion curve and higher predictive accuracy than for the left kidney.

Prediction Results for the Functional Curve (B): For the left kidney, MSE = 255.60, MAE = 15.46, and $R^2$ = -13.17, indicating substantial deviations and that the model fails to capture the left kidney's functional curve. For the right kidney, MSE = 55.45, MAE = 4.60, and $R^2$ = 0.99, indicating highly accurate prediction of the right kidney's functional curve by the model, with an ideal fitting effect.

Prediction Results for the Perfusion Curve (A): For the left kidney, the Mean Squared Error (MSE) was 21790.24, the Mean Absolute Error (MAE) was 123.93, and the coeffi-

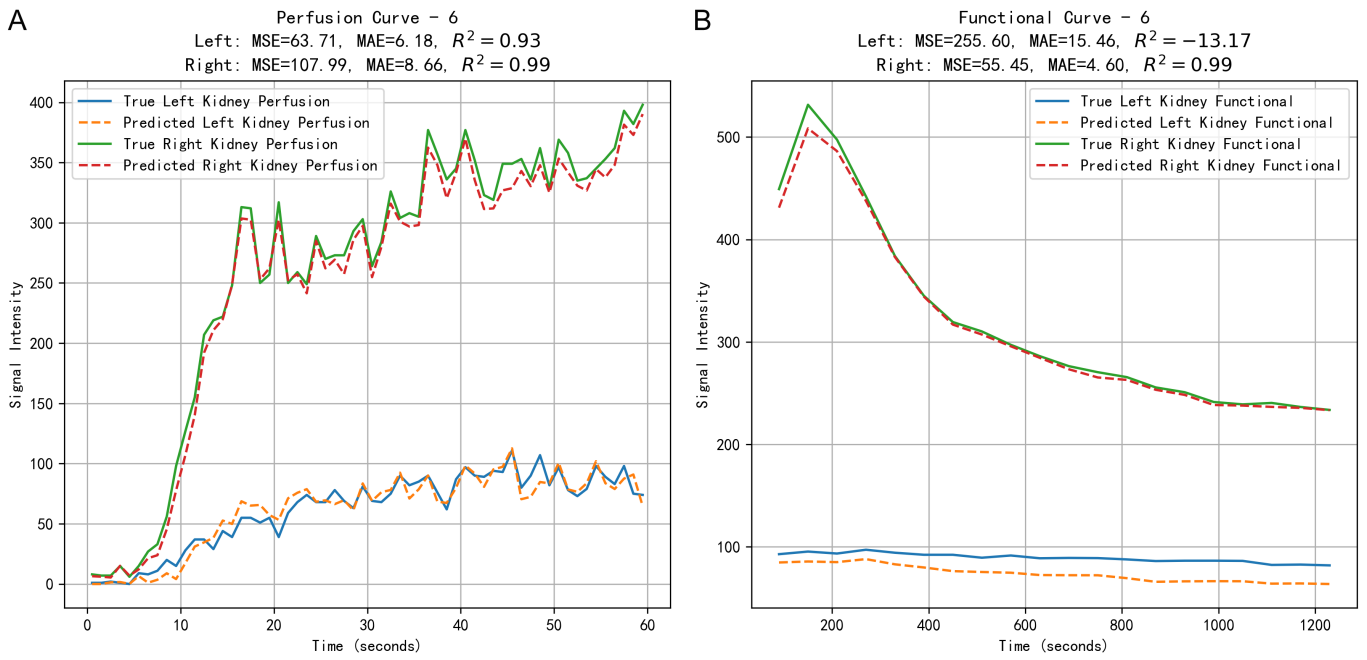


**Figure 1.** Comparison of actual time-activity curves and predicted curves of bilateral kidneys after injection extravasation (Sample 6). A: Renal blood perfusion curve (Sample 6). Blue line: actual left kidney curve; yellow dashed line: predicted left kidney curve; green line: actual right kidney curve. B: Renal blood perfusion curve (Sample 6). Blue line: actual left kidney curve; yellow dashed line: predicted left kidney curve; green line: actual right kidney curve.

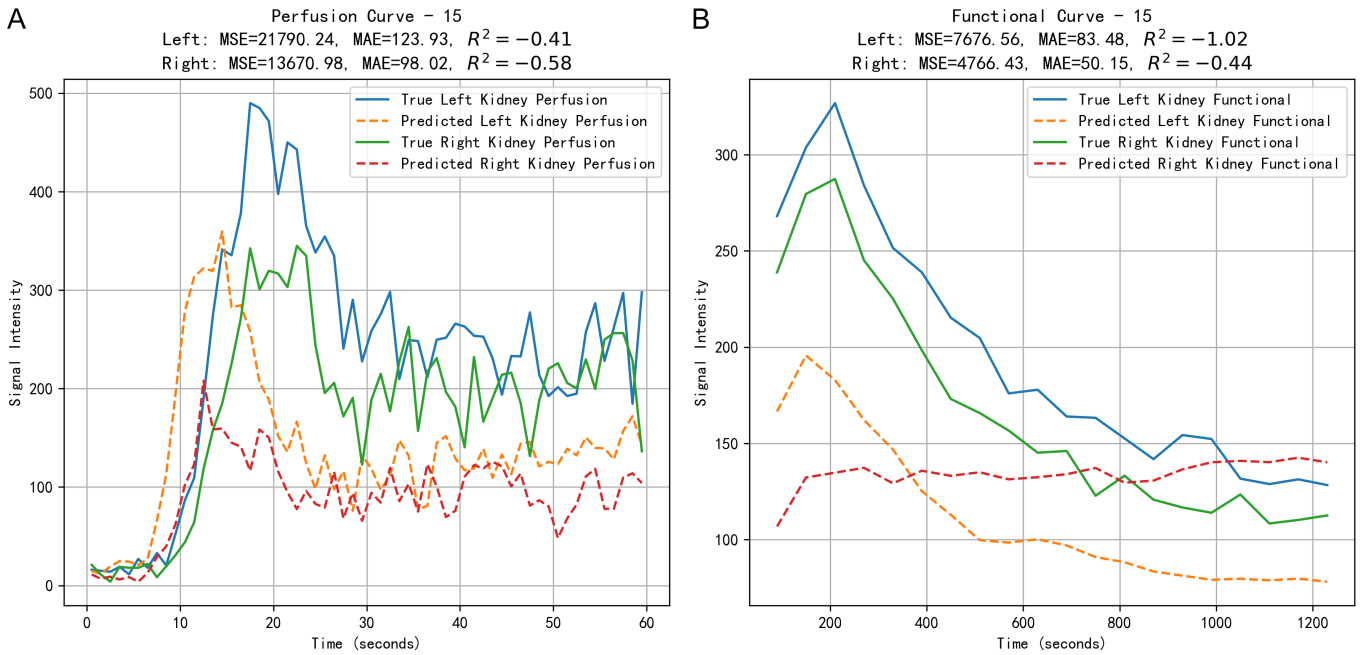


**Figure 2.** Comparison of actual time-activity curves and predicted curves of bilateral kidneys after injection extravasation (Sample 15). A: Renal blood perfusion curve (Sample 15). Blue line: actual left kidney perfusion curve; yellow dashed line: predicted left kidney curve; green line: actual right kidney curve; red dashed line: predicted right kidney curve. B: Renal functional curve (Sample 15). Blue line: actual left kidney perfusion curve; yellow dashed line: predicted left kidney curve; green line: actual right kidney curve; red dashed line: predicted right kidney curve.

cient of determination ($R^2$) was -0.41, indicating substantial discrepancy between the predicted and actual values in overall morphology. For the right kidney, the MSE was 13670.98, the MAE was 98.02, and the $R^2$ was -0.58, suggesting that the fluctuation trend of the predicted perfusion curve for the right kidney did not fully align with the true curve.

Prediction Results for the Functional Curve (B): For the left kidney, the MSE was 7676.56, the MAE was 83.48,

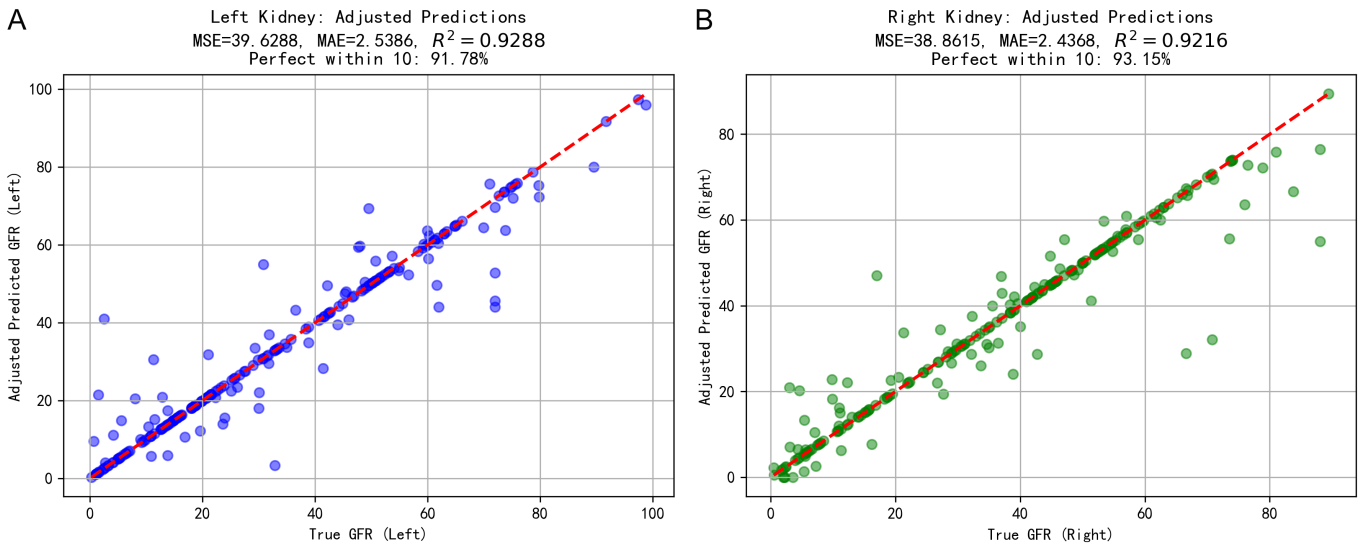


**Figure 3.** Comparison of corrected predicted GFR with actual GFR after injection extravasation in SPECT renal dynamic imaging. A: Comparison between the actual GFR and the predicted GFR after injection extravasation of the left kidney: most data points in the figure are mostly clustered along the reference line, with only a few showing deviations. B: For the right kidney, the actual GFR is compared with the predicted GFR during injection leakage in the graph, with most data points clustered along the line, while only a few deviate.

and the $R^2$ was -1.02. For the right kidney, the MSE was 4766.43, the MAE was 50.15, and the $R^2$ was -0.44. In the leakage curve prediction of Sample 15, all $R^2$ values were negative, indicating that the model exhibited limited performance in predicting the curves of both kidneys under contrast medium extravasation, and the model's predictive capability still has room for improvement.

*Prediction results of bilateral renal GFR after extravasation of SPECT renal dynamic imaging agent*

The mean $R^2$ values of the Transformer model for GFR prediction of the left and right kidneys were 0.85 and 0.88, respectively. The model demonstrated strong predictive capability. For the left kidney, the model achieved an $R^2$ of 0.9288, with 91.78% of predictions falling within a clinically acceptable tolerance of ±5 ml/min of the ground truth. Similarly, for the right kidney, the $R^2$ reached 0.9216, with an accuracy rate of 93.15% based on the same tolerance threshold. It is important to note that the ±5 ml/min criterion was used strictly as a statistical threshold to define 'clinical accuracy' (Success Rate) and did not involve any modification of the predicted values. For the left kidney, MSE = 39.6288 and MAE = 2.5386; for the right kidney, MSE = 38.8615 and MAE = 2.4368. Scatter plot demonstrated a strong correlation between predicted and actual values, with minimal boundary deviations (**Figure 3**).

## Discussion & clinical implementation and quality control

*Discussion*

With the rapid development of modern imaging technology, the incidence of Chronic Kidney Disease (CKD) and the detection rate of renal cell carcinoma have risen year by year. Surgical resection remains the only effective curative treatment for localized renal tumors. Therefore, accurate and comprehensive preoperative assessment of split renal function is critically important [13].

To address this issue, this study designed an integrated AI method based on the Transformer architecture, constructing a model to predict the time-activity curves and GFR values of bilateral kidneys after radionuclide extravasation during SPECT renal dynamic imaging. By incorporating a self-attention mechanism and leveraging multimodal inputs (renal dynamic curves, height, weight, serum creatinine, urea, and uric acid), the model achieved high-precision calibration of extravasation curves. The results showed that the model's calibration of renal extravasation curves was consistent with the expected trend, and the predicted GFR values were highly consistent with those obtained via the plasma clearance method, effectively improving the clinical efficiency and diagnostic accuracy of renal dynamic imaging.

Currently, AI-based approaches that extract information from medical images and construct predictive models for disease diagnosis and assessment have demonstrated increasing effectiveness [15]. For the calibration and prediction of renal extravasation curves (**Figure 1**), the Transformer model exhibited strong trend restoration capability, bringing the prediction of extravasation curves close to actual non-extravasation curves. However, in the late-stage prediction of functional curves, the predicted curves showed a flattening trend, with slight deviations from the dynamic changes in actual values. This indicates that the model's ability to capture long-term time series is limited, and there is room for improvement in modeling long-term temporal dependencies. Future work could

explore longer sequence inputs or hybrid architectures that integrate recurrent networks (for example, Long Short-Term Memory, LSTM) to enhance time-series modeling. For Sample 15 (**Figure 2**), the curve exhibited significant fluctuations, with deviations in mid-to-late-stage predictions. Although the overall trend was preserved, the amplitude error indicates a need for optimization. Extravasation correction focuses on trends and is more suitable for qualitative analysis, these results suggest that the model's robustness in complex extravasation scenarios requires improvement [16].

The Transformer model also achieved significant results in predicting GFR after injection extravasation in SPECT renal dynamic imaging. The mean $R^2$ values for the left and right kidneys were 0.85 and 0.88, respectively. Using a clinically acceptable error margin of ±5 ml/min, the prediction accuracy for both kidneys surpassed 90%. Scatter plot analysis (**Figure 3**) showed a strong correlation between predicted and actual values with minimal boundary deviations and an approximately normal distribution, indicating high predictive precision for GFR. Nevertheless, negative $R^2$ values were observed in individual samples, potentially due to inadequate sample size or suboptimal data quality. Therefore, in practical clinical applications, routine physician review is recommended [17].

Prior work has demonstrated the potential of Transformer-based models in clinical prediction. Ma et al [18] found that a Transformer-based prediction model could effectively evaluate lymph node metastasis in patients with lung adenocarcinoma; Wang et al [19] proposed a multi-modal Transformer model to predict sepsis within 36 hours of ICU admission; Bian et al [20] used a hybrid Transformer-LSTM model to achieve high accuracy in glucose prediction. Consistent with these studies, the present findings indicate that the Transformer can serve as a reliable approach for calibrating and predicting bilateral renal curves and GFR values after injection extravasation in SPECT renal dynamic imaging.

Regarding regional and healthcare system differences, this study has several limitations: (1) The retrospective design may limit the model's predictive value and generalizability; (2) Renal dynamic data were obtained from different devices; although standardized preprocessing was performed, it may still have adverse effects on the analysis results; (3) The sample size needs to be further expanded, which may lead to potential biases in model predictions. Future work should pursue large-scale, multi-center collaboration to collect more diverse data and consider integrating real-time imaging to enhance robustness [21]. Additional directions include increasing sample diversity, introducing attention mechanisms to better capture fluctuations, and computing additional metrics. Building on this research, a Transformer multi-modal fusion model could be used in future studies to predict long-acquisition renal function curves using early time points in SPECT renal dynamic imaging, thereby shortening scan time.

*Clinical implementation and quality control*

To safely integrate this model into the clinical workflow, we propose a 'Human-in-the-loop' protocol. Although the model performs well in the majority of cases, the observation of outliers (e.g., Sample 6) necessitates physician oversight. We recommend the following criteria for accepting AI-generated results:

Visual Inspection: The clinician must verify that the generated curve exhibits physiological morphology (smooth perfusion, uptake, and excretion phases) rather than chaotic fluctuations.

Consistency Check: The kinetics of the generated kidney curve should be logically consistent with the bladder curve.

If the AI output fails these visual checks, the standard of care remains to proceed with a physical re-examination. This ensures that the model serves as an efficiency-enhancing decision support tool without compromising patient safety.

## Conclusion

In conclusion, the multi-modal fusion Transformer model effectively calibrates and predicts outcomes after injection failure in SPECT renal dynamic imaging, demonstrating substantial potential to improve the efficiency and accuracy of renal dynamic imaging. The approach is expected to significantly reduce patients' radiation exposure, conserve medical resources, and provide an intelligent imaging framework to address the long-standing clinical problem of next-day re-examination after failed injection in SPECT renal dynamic imaging, thereby laying a solid foundation for clinical translation.

## Acknowledgements

This work was supported by (1) Science and Technology Program Project of Gansu Provincial Natural Science Foundation (grant number 25JRRA590). (2) Cuiying Scientific and Technological Innovation Program of Lanzhou University Second Hospital (grant numbers CY2022-QN-A19 and CY2022-QN-A11). (3) International science and technology cooperation project of Gansu Provincial Science and Technology Department (grant number 2023YFWA0009). (4) The Innovation and Entrepreneurship Project for Young Talents of Lanzhou Science and Technology Bureau (grant number 2023-4-18). (5) Gansu Province Youth Talent (Individual Project) (grant number 2026QNGR009).

## Disclosure of conflict of interest

None.

**Address correspondence to:** Jicheng Li and Jiangyan Liu, Department of Nuclear Medicine, Lanzhou University Second Hospital, Lanzhou 730030, Gansu, China. Tel: +86-139-19085864; E-mail: jchli19@lzu.edu.cn (JCL); Tel: +86-138-93669119; E-mail: ery_liujy@lzu.edu.cn (JYL); Zhen Cao, Siemens Healthineers Ltd., Shanghai 200120, China. Tel: +86-18721996493; E-mail: caozhenbangzhu@qq.com

## References

[1] Werner RA, Pomper MG, Buck AK, Rowe SP and Higuchi T. SPECT and PET radiotracers in renal imaging. Semin Nucl Med 2022; 52: 406-418.

[2] Nguyen DL, de Labriolle-Vaylet C, Durand E, Fernandez PX, Bonnin F, Deliu D, Besson FL and Chaumet-Riffaud P. Reproducibility of differential renal function measurement using technetium-99m-ethylenedicysteine dynamic renal scintigraphy: a French prospective multicentre study. Nucl Med Commun 2018; 39: 10-15.

[3] Sitek A, Gullberg GT, Di Bella EV and Celler A. Reconstruction of dynamic renal tomographic data acquired by slow rotation. J Nucl Med 2001; 42: 1704-1712.

[4] Tran TT, Yun G and Kim S. Artificial intelligence and predictive models for early detection of acute kidney injury: transforming clinical practice. BMC Nephrol 2024; 25: 353.

[5] Beytur MF, Kirli EA, Sahin KC, Kazanasmaz E, Sayman HB and Onal B. A novel method in conventional dynamic kidney scintigraphy: dynamic 99mTc-MAG3 SPECT/CT. Urology 2025; 199: 11-19.

[6] Li J, Huang L, Luo Y, Zhang K, Wang J, Feng J and Liu J. Inferences of SPECT renal dynamic imaging injection quality based on lung and abdominal aorta imaging features. Ann Nucl Med 2022; 36: 710-716.

[7] Brix G, Nekolla EA, Borowski M and NoRke D. Radiation risk and protection of patients in clinical SPECT/CT. Eur J Nucl Med Mol Imaging 2014; 41 Suppl1: S125-S136.

[8] Fedrigo R, Coope RJN, Chaussé G, Bloise I, Gowdy C, Bénard F, Rahmim A and Uribe CF. Development of lesion and organ negative cast modelling technique for quality assurance and optimization of nuclear medicine images. Commun Med (Lond) 2025; 5: 303.

[9] Miller ZA and Dwyer K. Artificial intelligence to predict chronic kidney disease progression to kidney failure: a narrative review. Nephrology (Carlton) 2025; 30: e14424.

[10] Zhou H, Zhang S and Peng J. Beyond efficient transformer for long sequence time-series forecasting. Proc AAAI Conf Intell 2021; 35: 11106-11115.

[11] Yuan J, Zhou F, Guo Z, Li X and Yu H. HCformer: hybrid CNN-transformer for LDCT image denoising. J Digit Imaging 2023; 36: 2290-2305.

[12] Zisser M and Aran D. Transformer-based time-to-event prediction for chronic kidney disease deterioration. J Am Med Inform Assoc 2024; 31: 980-990.

[13] Fani F, Regolisti G, Delsante M, Cantaluppi V, Castellano G, Gesualdo L, Villa G and Fiaccadori E. Recent advances in the pathogenetic mechanisms of sepsis-associated acute kidney injury. J Nephrol 2018; 31: 351-359.

[14] Hamouda M. Small urine leak after renal transplantation. Saudi J Kidney Dis Transpl 2019; 30: 564-570.

[15] Byeon Y, Park YW, Lee S, Park D, Shin H, Han K, Chang JH, Kim SH, Lee SK, Ahn SS and Hwang D. Interpretable multimodal transformer for prediction of molecular subtypes and grades in adult-type diffuse gliomas. NPJ Digit Med 2025; 8: 140.

[16] Wymer DC. Nuclear Renal Scan. StatPearls [Internet]. Treasure Island (FL): StatPearls Publishing; 2023. PMID: 33232048.

[17] Lanot A, Akesson A, Nakano FK, Vens C, Björk J, Nyman U, Grubb A, Sundin PO, Eriksen BO, Melsom T, Rule AD, Berg U, Littmann K, Åsling-Monemi K, Hansson M, Larsson A, Courbebaisse M, Dubourg L, Couzi L, Gaillard F, Garrouste C, Jacquemont L, Kamar N, Legendre C, Rostaing L, Ebert N, Schaeffner E, Bökenkamp A, Mariat C, Pottel H and Delanaye P. Enhancing individual glomerular filtration rate assessment: can we trust the equation? Development and validation of machine learning models to assess the trustworthiness of estimated GFR compared to measured GFR. BMC Nephrol 2025; 26: 47.

[18] Ma X, Xia L, Chen J, Wan W and Zhou W. Development and validation of a deep learning signature for predicting lymph node metastasis in lung adenocarcinoma: comparison with radiomics signature and clinical-semantic model. Eur Radiol 2023; 33: 1949-1962.

[19] Wang YQ, Zhao Y, Petzold L and Callcut R. Integrating physiological time series and clinical notes with transformer for early prediction of sepsis. arXiv:2203.14704.

[20] Bian Q, As'arry A, Cong X, Rezali KABM and Raja Ahmad RMKB. A hybrid transformer-LSTM model apply to glucose prediction. PLoS One 2024; 19: e0310084.

[21] Ponce D, de Andrade LGM, Claure-Del Granado R, Ferreiro-Fuentes A and Lombardi R. Development of a prediction score for in-hospital mortality in COVID-19 patients with acute kidney injury: a machine learning approach. Sci Rep 2021; 11: 24439.